






ORIGINAL RESEARCH

SerpinG1: A Novel Biomarker Associated With Poor Coronary Collateral in Patients With Stable Coronary Disease and Chronic Total Occlusion

Shuai Chen, MD*; Le-Ying Li, MD*; Zhi-Ming Wu, MD; Yong Liu, MD; Fei-Fei Li, PhD; Ke Huang, MD; Yi-Xuan Wang, MD; Qiu-Jing Chen , MD; Xiao-Qun Wang , MD, PhD; Wei-Feng Shen, MD, PhD; Rui-Yan Zhang, MD, PhD; Ying Shen, MD, PhD; Lin Lu , MD, PhD; Feng-Hua Ding , MD, PhD; Yang Dai , PhD

BACKGROUND: This study aimed to explore predictive biomarkers of coronary collateralization in patients with chronic total occlusion.

METHODS AND RESULTS: By using a microarray expression profiling program downloaded from the Gene Expression Omnibus database, weighted gene coexpression network analysis was constructed to analyze the relationship between potential modules and coronary collateralization and screen out the hub genes. Then, the hub gene was identified and validated in an independent cohort of patients (including 299 patients with good arteriogenic responders and 223 patients with poor arteriogenic responders). Weighted gene coexpression network analysis showed that *SERPING1* in the light-cyan module was the only gene that was highly correlated with both the gene module and the clinical traits. Serum levels of serpinG1 were significantly higher in patients with bad arteriogenic responders than in patients with good arteriogenic responders (472.53 ± 197.16 versus 314.80 ± 208.92 $\mu\text{g/mL}$; $P < 0.001$) and were negatively associated with the Rentrop score (Spearman $r = -0.50$; $P < 0.001$). Receiver operating characteristic curve analysis indicated that the area under the curve was 0.77 (95% CI, 0.72–0.81; $P < 0.001$) for serum serpinG1 in prediction of bad arteriogenic responders. After adjusting for traditional cardiovascular risk factors, serum serpinG1 levels (per SD) remained an independent risk factor for bad arteriogenic responders (odds ratio, 2.20 [95% CI, 1.76–2.74]; $P < 0.001$).

CONCLUSIONS: Our findings illustrate that *SERPING1* screened by weighted gene coexpression network analysis was associated with poor collateralization in patients with chronic total occlusion.

Key Words: chronic total occlusion ■ coronary artery disease ■ coronary collateralization ■ weighted gene coexpression network analysis

Chronic total occlusion (CTO) is characterized by complete coronary artery stenosis without antero-grade flow for at least 3 months and represents the most advanced form of coronary artery disease.¹ In the presence of severe obstructive or occluded coronary

lesions, coronary collateralization is an important compensatory mechanism for myocardial ischemia and improves symptoms and quality of life because it can provide additional blood supply to rescue the ischemic region of the myocardium.^{2–4} Abundant evidence suggests

Correspondence to: Yang Dai, PhD, Feng-Hua Ding, MD, PhD, or Lin Lu, MD, PhD, Department of Vascular and Cardiology, Rui Jin Hospital, 197 Rui Jin Rd II, Shanghai 200025, China. Email: yutongwushe@163.com; ruijindfh@126.com; rjulin1965@163.com

*S. Chen and L.Y. Li contributed equally.

Supplemental Material is available at <https://www.ahajournals.org/doi/suppl/10.1161/JAHA.122.027614>

For Sources of Funding and Disclosures, see page 10.

© 2022 The Authors. Published on behalf of the American Heart Association, Inc., by Wiley. This is an open access article under the terms of the [Creative Commons Attribution-NonCommercial](https://creativecommons.org/licenses/by-nc/4.0/) License, which permits use, distribution and reproduction in any medium, provided the original work is properly cited and is not used for commercial purposes.

JAHA is available at: www.ahajournals.org/journal/jaha

CLINICAL PERSPECTIVE

What Is New?

- This study performed weighted gene coexpression network analysis using a publicly available gene expression data set (GSE7547) to find SERPING associated with collateral circulation and validated it in an independent cohort.
- This study identified serpinG1 as an independent risk factor for poor collateralization in patients with stable angina and chronic total occlusion.

What Are the Clinical Implications?

- As a novel risk factor, serpinG1 may facilitate the identification of poor collateral formation in patients with stable angina and chronic total occlusion.
- Because intravenous plasma-derived serpinG1 (Cinryze) and subcutaneous treatments with plasma-derived serpinG1 are approved for hereditary angioedema-targeted therapy, this study also suggests that patients with stable coronary disease who supplement with serpinG1 for therapeutic purposes need to be more carefully assessed for their clinical benefit.

Nonstandard Abbreviations and Acronyms

BAR	bad arteriogenic responder
CTO	chronic total occlusion
DEG	differentially expressed gene
GAR	good arteriogenic responder
GO	Gene Ontology
WGCNA	weighted gene coexpression network analysis

that patients with well-developed collateral vessels have lower rates of cardiac mortality and major adverse cardiac events than those without collateral vessels.^{5–9} In adults, coronary collateral development has been postulated to occur through a combination of angiogenesis and arteriogenesis.^{10,11} Angiogenesis and arteriogenesis are regulated by multiple clinical and biochemical factors, inflammatory cytokines, and growth factors.^{3,12,13} Despite increasing putative angiogenic and arteriogenic factors, the benefits of medical therapies based on these factors to improve ischemic tissue perfusion are limited.

In recent years, with the remarkable evolution of systems biology, extensive microarray data have been used to identify hub genes and crucial pathways involved in collateralization. Systems biology focuses on the concerted regulation of whole gene networks, which may lead to greater insight into the physiology of collateral development. Weighted gene coexpression

network analysis (WGCNA) is a highly used systems biology algorithm used to analyze gene expression and clinical traits.^{14,15} The hierarchical clustering function of WGCNA can discover modules comprising highly correlated genes, identify gene module-trait relationships, and extract important genes from biologically meaningful modules. Consequently, WGCNA can be used to investigate hub genes closely related to clinical traits, which will provide us with the hope of discovering new molecular biomarkers involved in collateral development.

In the present study, we aimed to identify susceptible modules and hub genes associated with the formation of collateral coronary arteries by establishing a WGCNA algorithmic model and to provide novel noninvasive biomarkers by analyzing serum levels of candidate genes from patients with complete coronary occlusion with good or poor collaterals.

METHODS

The microarray data set used for WGCNA was downloaded from the Gene Expression Omnibus database of the National Center of Biotechnology Information (GSE7547), and the remaining data and materials that support the findings of this study are available from the corresponding author on reasonable request.

Acquiring and Preprocessing the Microarray Data

The microarray data set and clinical traits were downloaded from the Gene Expression Omnibus database of the National Center of Biotechnology Information. We used the GSE7547 data set to identify the relationship between changes in hub gene expression and the degree of coronary collateral artery formation.¹⁶ GSE7547 was based on the platform of the GPL5104 Sentrix HumanRef-8 v2 Expression BeadChip and collected circulating cells from patients scheduled for percutaneous coronary intervention for coronary artery disease.¹⁶ All patients underwent coronary angiography to distinguish between good arteriogenic responders (GARs) and bad arteriogenic responders (BARs). For patients with multiple technical replicates, the average quantity was used as the expression value. Finally, we used the resting monocyte expression profile to identify the relationship between changes in hub genes and the formation of coronary collateral arteries from GARs (n=18) and BARs (n=19).

Identification of Differentially Expressed Genes

After data were normalized, and the differentially expressed genes (DEGs) between the BARs and GARs were analyzed using the R package limma (version

4.1.1), as described previously.^{17,18} The fold change of all genes was log₂ transformed to normalize the expression level, and the *P* value was adjusted using the Benjamini-Hochberg method. The gene with absolute log₂ fold change >0.25 and *P*<0.05 was considered as a significant DEG.

Construction of the Weighted Gene Coexpression Network

In our study, we constructed a gene coexpression network using the standard WGCNA procedure.¹⁴ After the gene expression data were obtained, the top 25% of genes with high expression variance were selected for analysis. The Pearson correlation coefficient between any 2 genes was calculated using a pairwise correlation matrix to construct a gene coexpression network. Following this, the Pearson correlation matrix was switched to an adjacency matrix with the proper power value when the scale-free *R*² was first >0.90. Subsequently, the topological overlap matrix was converted using the `blockwiseModules` function in the R software with the following parameters: `minClusterSize=50`, and `power=7`. Then, a clustering dendrogram was constructed and visualized using the `plotDendroAndColors` function, and the branches of the clustering tree were merged into different gene modules using the dynamic tree-cutting algorithm.¹⁵ Different gene modules were represented by different colors. Genes that could not be included in any module were classified into the gray module and removed in subsequent analysis.

We performed Pearson correlation tests to assess the correlation between modules and clinical features to find the meaningful modules. For each module, we defined a quantitative measure of module membership as the correlation of the module eigengene, gene expression profile, and correlation of the gene and clinical trait as gene significance. We performed further analyses of the genes included in the meaningful modules with the highest module membership and gene significance values.

Functional Enrichment Analysis

The DEGs in the modules of interest were selected and functionally analyzed using the Gene Ontology (GO) database. GO annotations were divided into 3 categories: molecular functions, biological processes, and cellular components. The `clusterProfiler` package in R software was used to perform GO analyses, as described previously.¹⁹

Study Population

A total of 634 consecutive patients with stable angina and CTO (>3 months) of at least 1 major epicardial coronary artery between March 2018 and October 2021 were screened from the database of the Shanghai

Rui Jin Hospital Percutaneous Coronary Intervention Outcomes Program. Stable angina was diagnosed according to the criteria recommended by the American College of Cardiology/American Heart Association.²⁰ The duration of coronary occlusion was estimated on the basis of information obtained from a previous angiogram, a history of myocardial infarction in the area of the myocardium supplied by the occluded vessel, or the first onset of an abrupt worsening of existing angina pectoris. For this study, 112 patients were excluded because of a history of coronary artery bypass grafting (*n*=29), percutaneous coronary intervention within the past 3 months (*n*=38), chronic heart failure with New York Heart Association class III or IV (*n*=15), pulmonary heart disease (*n*=12), renal failure requiring hemodialysis (*n*=4), immune system disorders or malignant tumor (*n*=7), and type 1 diabetes (*n*=7) as these conditions could impact collateral formation. A total of 522 patients were included in the final analysis. This analysis was approved by the Ruijin Hospital and Shanghai Jiao Tong University School of Medicine Ethics Committee (RJH20140311), and written informed consent was obtained from all patients.

Coronary Angiography

Coronary angiography was performed through the femoral or radial artery using 6F diagnostic catheters. Quantitative coronary angiography was independently performed by 2 experienced cardiologists who were blinded to the study protocol and biochemical measurements. The degree of coronary collateralization supplying the distal area of the total coronary occlusion was visually graded using the Rentrop scoring system as follows: 0=no visible collaterals; 1=poorly opacified collaterals with faint visualization of the distal vessel; 2=partial filling of the collateral vessels; and 3=complete filling of the collateral vessels. Patients were then classified as BARs (Rentrop scores of 0 and 1) or GARs (Rentrop scores of 2 and 3), according to the Rentrop score.²¹ In case of disagreement, any difference in interpretation was resolved by the third reviewer.

Biochemical Studies

Blood samples were obtained from all patients on the day of angiography after overnight fasting. Blood plasma samples were collected and stored at -80 °C before analysis. Serum levels of glucose, creatinine, urine urea nitrogen, triglyceride, total cholesterol, low-density lipoprotein cholesterol, and high-density lipoprotein cholesterol were assessed using a standard laboratory protocol (HITACHI 912 Analyzer; Roche Diagnostics, Germany). Glomerular filtration rate (GFR) was estimated using the Chronic Kidney Disease Epidemiology Collaboration equation: $GFR (mL/min \text{ per } 1.73m^2) = 141 \times \min(\text{creatinine}/k, 1) \alpha \times \max(\text{creatinine}/k,$

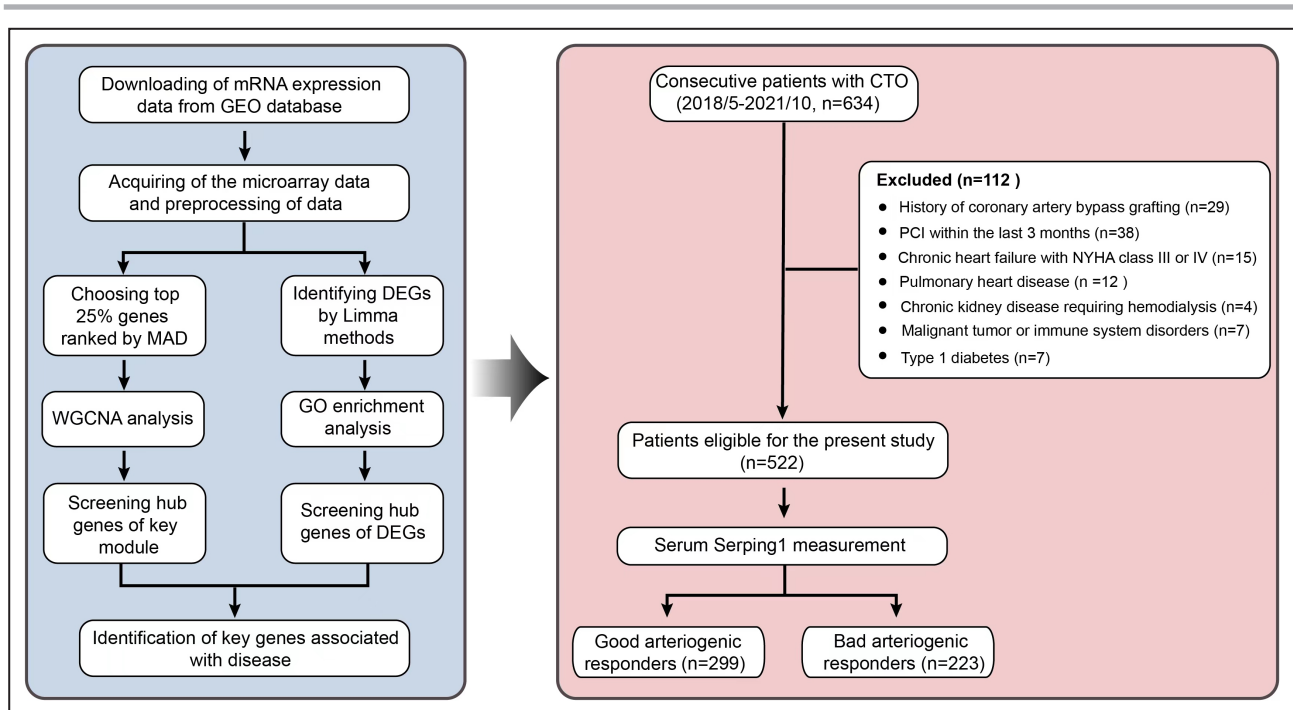


Figure 1. Flowchart describing the schematic overview of the current study design.

We used the GSE7547 data set to identify the relationship between changes in hub genes expressed on monocytes and the degree of coronary collateral artery formation. After data processing, the light-cyan module was identified as the most significant module through the WGCNA. DEGs in the light-cyan module were analyzed using the limma package of R. GO enrichment analysis was performed on DEGs in the light-cyan module. Finally, the hub gene *SERPING1* was identified and validated in an independent cohort of patients. CTO indicates chronic total occlusion; DEGs, differentially expressed genes; GEO, Gene Expression Omnibus; GO, Gene Ontology; MAD, median absolute deviation; NYHA, New York Heart Association; PCI, percutaneous coronary intervention; and WGCNA, weighted gene coexpression network analysis.

1) $-1.209 \times 0.993 \text{age} \times 1.018$ (if female sex), where k is 0.7 for female patients and 0.9 for male patients, α is -0.329 for female patients and -0.411 for male patients, \min indicates the minimum creatinine/ k or 1, and \max indicates the maximum creatinine/ k or 1.²²

Serum levels of serpinG1 were measured via a commercially available ELISA kit, according to the manufacturer's instructions (CSB-EL021086HU; CUSABIO). The detection range of the kit was 18.75 to 1200 ng/mL, and the sensitivity of the kit was 4.7 ng/mL. As for the precision of the kit, the average intra-assay coefficient of variance and the average interassay coefficient of variance were $<8\%$ and 10% , respectively. The serum samples were diluted 1:1000 with dilutant buffer before performing the detection. The optical density of each sample was determined using a microplate reader at 450 nm. The levels of serpinG1 were calculated using the optical density values of the standard curve.

Statistical Analysis

In our study, continuous variables are presented as the mean \pm SD and median (25th–75th percentile) for normal and nonnormal distributions, respectively, and categorical data are summarized as frequencies (percentages). The differences between groups for

continuous variables and categorical variables were analyzed using the Student t -test and χ^2 test, respectively. Pearson and Spearman correlation analyses were performed as appropriate. We constructed multivariable logistic regression models to assess the independent determinants of poor collateralization without (model 1) and with (model 2) serpinG1. Receiver operating characteristic curve analyses were performed with serum serpinG1 and predicted probabilities (C statistic) for BARs derived from regression models with and without serpinG1. The areas under the curves were compared using the DeLong method with MedCalc software for Windows (version 11.4; Mariakerke, Belgium). All analyses used 2-sided tests with an overall significance level (α) of 0.05, and all tests were performed using R software (version 4.1.1) and SPSS 25.0 for Windows (SPSS, Inc, Chicago, IL).

RESULTS

Data Preprocessing

We set up a workflow, as seen in Figure 1, to identify diagnostic biomarkers for BARs in patients with coronary artery disease. We used the GSE7547 data set to identify the relationship between changes in hub

genes expressed on monocytes and the degree of coronary collateral artery formation. In this database, there were 48 resting, unstimulated monocyte samples from patients with BARs and GARs. For patients with multiple technical replicates, the average quantity was used as the expression value. The remaining samples (n=37) were clustered by the average linkage method. On the basis of these results, we excluded one outlier sample and included 36 samples for further analysis (Figures S1 and S2A).

Construction of Weighted Gene Coexpression Networks

WGCNA methods were applied to explore the causal genes of the disease using the expression profile with the highest 25% variance. In summary, 18 GAR and

18 BAR samples with 6398 gene expression profiles were included in the WGCNA. Before constructing the weighted coexpression network, we selected an appropriate power value to balance scale independence and mean connectivity of the gene module. After calculation, we found that the scale independence was >0.90 and had a higher mean connectivity when the power value was equal to 7 (Figure S2B and S2C). By calculating the scale-free topology fitting index, the value of R^2 reached 0.9 (Figure S2D and S2E). Thus, the power value was selected as 7 in the following analysis. As a result, we obtained a hierarchical clustering tree, and an aggregate of 16 coexpression modules was established for further analysis. The number of genes in these modules ranged from 56 to 1160 (Figure S3A). Genes whose expression levels

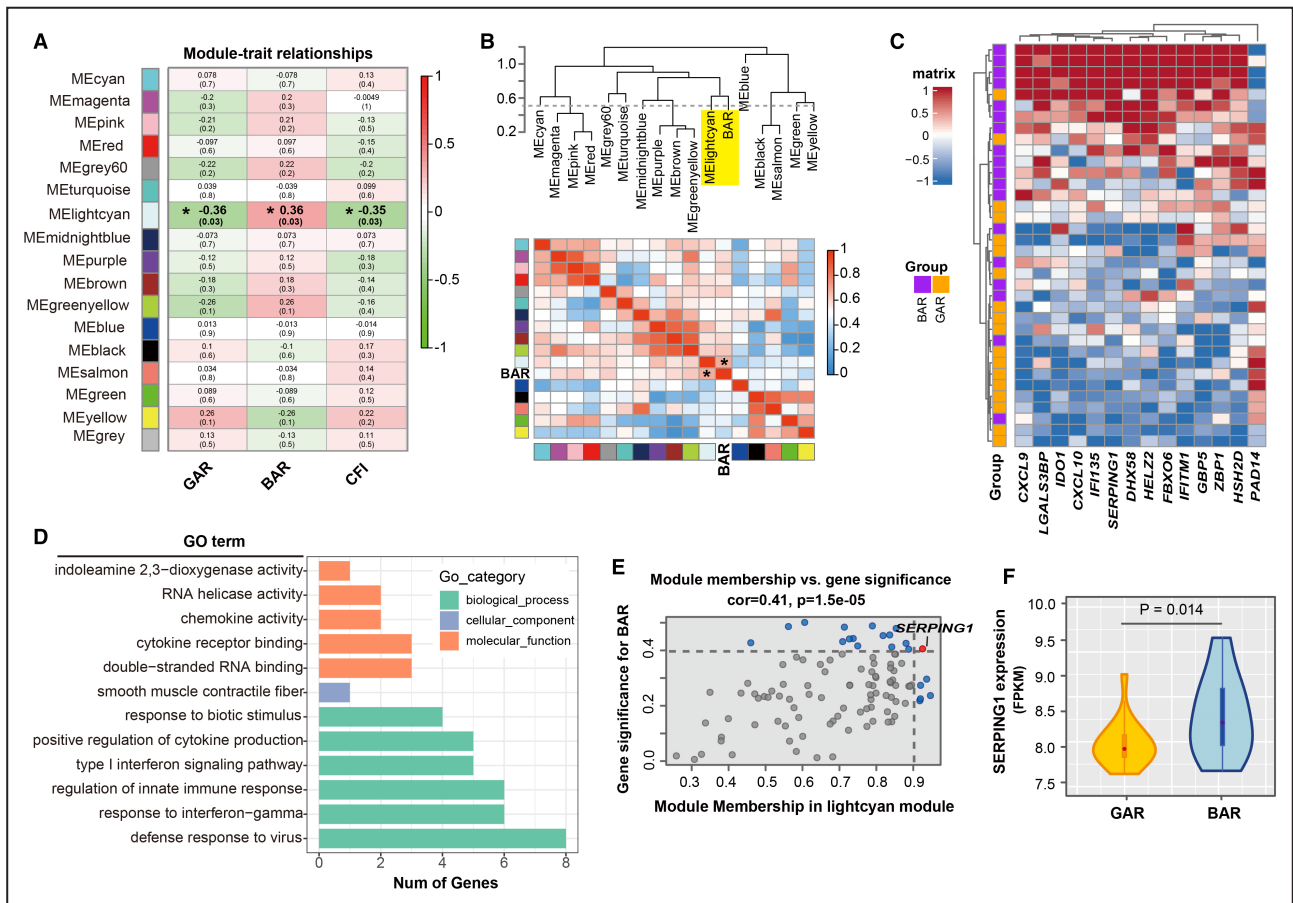


Figure 2. Identification and functional enrichment analysis of hub genes.

A, Heat map of the correlation between clinical traits, including GARs, BARs, and CFI. Each column corresponds to a clinical trait, and each row corresponds to a module. Each box contains the corresponding correlation coefficient and P value. Green represents negative correlation, and red represents positive correlation. **B**, Eigengene adjacency heat map showing extramodular connectivity among all the modules and clinical traits. Red indicates high adjacency (positive correlation), and blue indicates low adjacency (negative correlation). **C**, Heat map of the DEGs in the light-cyan module. The expression level of each gene in one sample is represented in the shade of red or blue, which represents upregulation and downregulation, respectively. **D**, The top GO terms enriched by 14 DEGs in the light-cyan module. **E**, Correlation between MM of modules of interest and GS with clinical traits. Scatterplot of GS for BARs vs MM in the light-cyan module. **F**, Violin plot of the expression level of *SERPING1*. The orange violin represents the GAR group as control, and the blue violin represents the BAR group. BARS indicates bad arteriogenic responders; CFI, collateral flow index; DEGs, differentially expressed genes; GARs, good arteriogenic responders; GO, Gene Ontology; GS, gene significance; ME, Module eigengene E; and MM, module membership.

could not be contained in any module were assigned to the gray modules and eliminated for further analysis. A topological overlap matrix was built to analyze the independence of the 16 coexpression modules. As described in the topological overlap matrix, a light color indicated high overlap, whereas dark colors indicated low overlap. On the basis of the topological overlap matrix, there were no significant differences among the 16 coexpression modules (Figure S3B).

Correlation Between Modules and Identification of Key Modules

In this study, the clinical features were provided by the GSE7547 profile in the Gene Expression Omnibus database. First, the correlation between genes and associated traits in the module was validated using an eigengene dendrogram and an eigengene adjacency heat map. As shown in the results, genes in the light-cyan module were significantly associated with the occurrence of BARs (Figure 2A). Module-trait associations were analyzed by correlating module sample eigengenes with clinical traits to identify significant associations. Only 1 module, the light-cyan module, was significantly correlated with BARs ($r=0.36$; $P=0.03$) (Figure 2B). A scatterplot showing the gene significance for BARs versus module membership in the light-cyan module indicated that the light-cyan module was significantly positively correlated with BARs ($r=0.41$; $P=1.5e-05$) (Figure 2E). In summary, we identified the light-cyan module as the most significant module for the occurrence of poor collateral formation.

Identification and Functional Enrichment Analysis of Hub Genes

We performed a more detailed analysis of the light-cyan module to identify hub genes associated with poor collateral formation. DEGs in the light-cyan module were analyzed using the limma package of R, as described previously. A total of 14 DEGs with absolute log₂ fold change >0.25 and $P<0.05$ were identified (Figure 2C). GO enrichment analysis was performed on the DEGs in the light-cyan module to better understand the modules associated with the collateral formation genotype. We found that these DEGs were mainly involved in the interferon- γ response, smooth muscle contraction, and cytokine receptor binding (Figure 2D). To identify hub genes that are associated with poor collateral formation, 3 criteria were applied, which included the following: (1) the candidate gene is particularly relevant to both module and clinical traits; (2) mRNA expression of this gene is different between the 2 groups; and (3) the gene must be a secreted protein to detect easily and has multiple biological functions. In our study, we

Table 1. Baseline Demographic and Clinical Characteristics in Patients With BARs and GARs

Characteristic	GARs (n=299)	BARs (n=223)	P value
Male sex, n (%)	250 (83.6)	164 (73.5)	0.005
Age, y	62.86 \pm 10.67	64.97 \pm 11.11	0.029
Body mass index, kg/m ²	24.95 \pm 3.19	25.23 \pm 3.66	0.361
Hypertension, n (%)	214 (71.6)	140 (62.8)	0.033
Diabetes, n (%)	135 (45.2)	134 (60.1)	0.001
Cigarette smoking, n (%)	88 (29.4)	85 (38.1)	0.037
Dyslipidemia, n (%)	68 (22.7)	65 (29.1)	0.097
Systolic blood pressure, mmHg	136.24 \pm 19.76	133.88 \pm 26.46	0.243
Diastolic blood pressure, mmHg	77.29 \pm 11.99	77.02 \pm 12.31	0.805
Fasting blood glucose, mmol/L	6.25 \pm 2.09	6.71 \pm 2.50	0.023
HbA1c, %	6.37 \pm 1.09	6.76 \pm 1.63	0.001
Serum creatinine, μ mol/L	88.61 \pm 44.77	98.61 \pm 64.82	0.038
Serum uric acid, μ mol/L	377.90 \pm 105.37	367.34 \pm 115.63	0.279
GFR, mL/min per 1.73m ²	80.80 \pm 18.18	76.23 \pm 23.92	0.014
Triglyceride, mmol/L	1.68 \pm 0.96	1.82 \pm 1.27	0.140
Total cholesterol, mmol/L	4.13 \pm 1.14	4.31 \pm 1.34	0.094
HDL cholesterol, mmol/L	1.04 \pm 0.25	1.02 \pm 0.22	0.362
LDL cholesterol, mmol/L	2.51 \pm 1.00	2.68 \pm 1.19	0.075
Apolipoprotein A, g/L	1.13 \pm 0.21	1.13 \pm 0.20	0.839
Apolipoprotein B, g/L	0.84 \pm 0.24	0.87 \pm 0.29	0.168
Lipoprotein (a), g/L	0.33 \pm 0.52	0.27 \pm 0.24	0.116
hs-CRP, mg/L	1.60 (0.60–4.32)	2.75 (0.85–6.77)	<0.001
Severity of CAD, n (%)			
1 Vessel	43 (14.4)	36 (16.1)	0.578
2 Vessels	88 (29.4)	56 (25.1)	0.275
3 Vessels	168 (56.2)	131 (58.7)	0.559
Medication, n (%)			
Antiplatelet	223 (74.6)	170 (76.2)	0.665
ACEIs/ARBs/ARNIs	182 (60.9)	137 (61.4)	0.896
β -Blockers	149 (49.8)	106 (47.5)	0.603
Calcium channel blockers	75 (25.1)	59 (26.5)	0.722
Statins	218 (72.9)	154 (69.1)	0.336
serpinG1, μ g/mL	314.80 \pm 08.92	472.53 \pm 197.16	<0.001

Values are given as mean \pm SD, median (25th–75th percentile), or number (percentage). ACEI indicates angiotensin-converting enzyme inhibitor; ARB, angiotensin receptor blocker; ARNI, angiotensin receptor–neprilysin inhibitor; BAR, bad arteriogenic responder; CAD, coronary artery disease; GAR, good arteriogenic responder; GFR, glomerular filtration rate; HbA1c, glycated hemoglobin; HDL, high-density lipoprotein; hs-CRP, high-sensitivity C-reactive protein; and LDL, low-density lipoprotein.

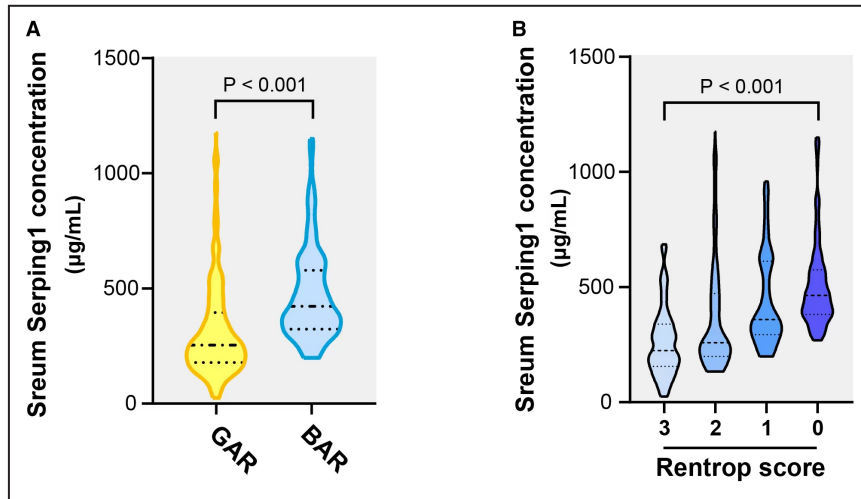


Figure 3. The relationship between plasma serpinG1 levels and coronary collateralization.

A, Serum levels of serpinG1 were significantly higher in patients with BARs than those in patients with GARs. **B**, The serum levels of serpinG1 increased stepwise according to the decrease in the Rentrop score. BARS indicates bad arteriogenic responders; and GARs, good arteriogenic responders.

found that SERPING1 met these criteria. In the scatterplot, we found that serpinG1 was the only gene with a module membership >0.9 and a gene significance >0.41 in the light-cyan module (Figure 2E). Moreover, the expression of serpinG1 was expressed higher in patients with BARs than in those with GARs (8.43 ± 0.56 versus 8.04 ± 0.32 FPKM; $P = 0.014$) (Figure 2F). Finally, serpinG1 seems to be one of the most abundant protease inhibitors in the blood circulation, which is known to regulate coagulation, complement, and contact (kallikrein-kinin enzyme) system activation.²³ Therefore,

we speculated that serpinG1 might play a critical role in poor collateral growth.

Validation of Hub Gene in an Independent Patient Cohort

The serum levels of serpinG1 were analyzed using ELISA in an independent patient cohort to confirm the main conclusion obtained from the microarray analysis. In this cohort, patients with BARs were mostly older individuals and women, had a history of cigarette

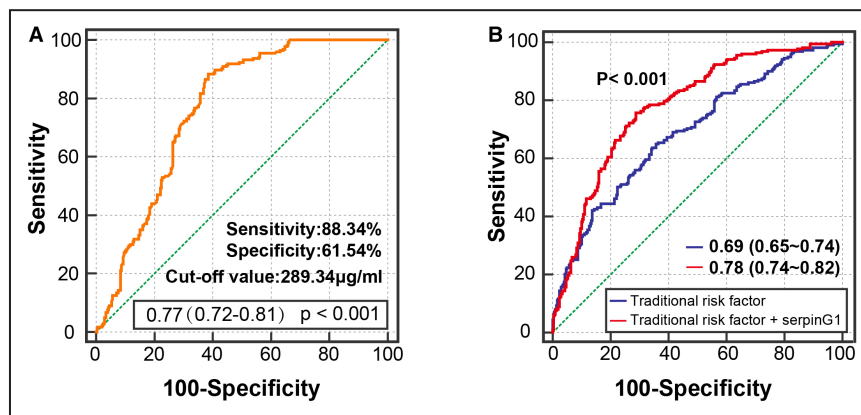


Figure 4. ROC curve analysis for detecting poor collateral growth.

A, ROC curves of plasma serpinG1 for diagnosing coronary collateralization. **B**, Predicted probabilities derived from regression models for detecting bad arteriogenic responders. Traditional risk factors include variables of male sex, age, body mass index, hypertension, diabetes, cigarette smoking, total cholesterol/high-density lipoprotein cholesterol ratio, glomerular filtration rate, and log-transformed hs-CRP. hs-CRP indicates high-sensitivity C-reactive protein; and ROC, receiver operating characteristic.

smoking and diabetes, and exhibited higher serum levels of blood glucose, glycosylated hemoglobin, creatinine, and hs-CRP (high-sensitivity C-reactive protein) but had a lower percentage of hypertension and a lower GFR than those with GARs (for all comparisons, $P < 0.05$). However, there were no significant differences between the 2 groups in terms of the body mass index, history of dyslipidemia, brachial blood pressure, the severity of coronary artery disease, or lipid profiles and medical treatments (for all comparisons, $P > 0.05$) (Table 1).

Serum levels of serpinG1 were significantly higher in patients with BARs than those in patients with GARs (472.53 ± 197.16 versus $314.80 \pm 208.92 \mu\text{g/mL}$; $P < 0.001$) (Figure 3A). The serum levels of serpinG1 increased stepwise according to the decrease in the Rentrop score (all $P < 0.05$) (Figure 3B). Moreover, serum levels of serpinG1 were negatively associated with the Rentrop score (Spearman $r = -0.50$; $P < 0.001$). After adjusting for male sex, age, body mass index, hypertension, diabetes, cigarette smoking, total cholesterol/high-density lipoprotein cholesterol ratio, GFR, and log-transferred hs-CRP, the serum levels of serpinG1 still correlated with the Rentrop score (Spearman $r = -0.38$; $P < 0.001$). Receiver operating characteristic curve analysis indicated that the area under the curve was 0.77 (95% CI, 0.72–0.81; $P < 0.001$) for serum serpinG1 in prediction of BARs, with an optimal cutoff point of $289.34 \mu\text{g/mL}$ (sensitivity=88.34%, and specificity=61.54%) (Figure 4A).

Multivariable logistic regression analysis was performed to analyze the association between serpinG1 and BARs. After adjusting for male sex, age, body mass index, hypertension, diabetes, cigarette smoking, total cholesterol/high-density lipoprotein cholesterol ratio, GFR, and log-transferred hs-CRP, serum levels of serpinG1 (per SD) remained an independent risk factor for BARs (odds ratio, 2.20 [95% CI, 1.76–2.74]; $P < 0.001$) (Table 2). The additional inclusion of serum levels of serpinG1 provided a significantly improved goodness of fit and predictive performance with an increase in Nagelkerke R^2 of 12.6% ($P < 0.001$) and C statistic of 0.090 (95% CI, 0.055–0.12; $P < 0.001$) (Figure 4B).

In the subgroup analysis, the diagnostic value of serpinG1 (per SD) for detecting BARs was consistent (P interaction ≥ 0.11) in all patient subgroups (Figure 5).

DISCUSSION

In the present study, we built a coexpression module using WGCNA and identified *SERPING1* as the hub gene with poor coronary collateralization. This study also demonstrated that increased serum serpinG1 levels were inversely associated with the degree of coronary collateralization in patients with stable angina and CTO.

In our study, we used WGCNA to analyze genes potentially associated with collateral formation, and

identified the light-cyan module as a significantly relevant cluster to poor coronary collateralization in patients with CTO. GO analyses on this module demonstrated that both the type 1 interferon response and interferon- γ signaling pathway were enriched during the inhibition of collateralization. Accumulating evidence suggests that interferon is a crucial inhibitor of collateralization.^{24–26} The high enrichment of interferon signals in the light-cyan module was consistent with a previous report,¹⁶ which proved the rationality of this WGCNA model from the side. In addition to the interferon-related genes *IFITM1* and GBP (guanylate-binding protein) family (GBP1, GBP4, and GBP5), the poor collateral-associated susceptibility genes in the light-cyan module also included CXCL10 (C-X-C motif chemokine ligand 10) and SERPING1. CXCL10 is an interferon-inducible chemokine best known for its chemoattractant effect on T cells and leukocytes and has previously been shown to have controversial angiostatic properties.²⁷ For serpinG1, despite being the only gene highly correlated with both gene module and clinical traits (poor coronary collateralization) in our WGCNA model, the association between serpinG1 and collateralization has never been reported before. Therefore, we assayed serum serpinG1

Table 2. Multivariate Logistic Regression Analyses for Poor Collateral Growth in Patients With Coronary Artery Disease

Variables	OR (95% CI)	P value
Model 1		
Male sex	0.50 (0.31–0.80)	0.004
Age (per 10 y)	1.26 (1.03–1.55)	0.022
Body mass index	1.06 (1.00–1.12)	0.048
Hypertension	0.59 (0.39–0.88)	0.010
Diabetes	1.66 (1.14–2.40)	0.008
Smoking	2.21 (1.44–3.39)	<0.001
Total cholesterol/HDL cholesterol ratio	1.12 (0.99–1.27)	0.082
GFR	0.99 (0.98–1.00)	0.058
Log-transferred hs-CRP	1.16 (1.06–1.27)	0.001
Model 2		
Male sex	0.52 (0.31–0.86)	0.011
Age (per 10 y)	1.22 (0.98–1.51)	0.070
Body mass index	1.06 (0.99–1.12)	0.075
Hypertension	0.61 (0.40–0.93)	0.023
Diabetes	1.52 (1.02–2.25)	0.038
Smoking	1.85 (1.17–2.91)	0.008
Total cholesterol/HDL cholesterol ratio	1.10 (0.96–1.26)	0.176
GFR	0.99 (0.98–1.00)	0.020
Log-transferred hs-CRP	1.18 (1.07–1.30)	0.001
serpinG1 (per SD)	2.20 (1.76–2.74)	<0.001

GFR indicates glomerular filtration rate; HDL, high-density lipoprotein; hs-CRP, high-sensitivity C-reactive protein; and OR, odds ratio.

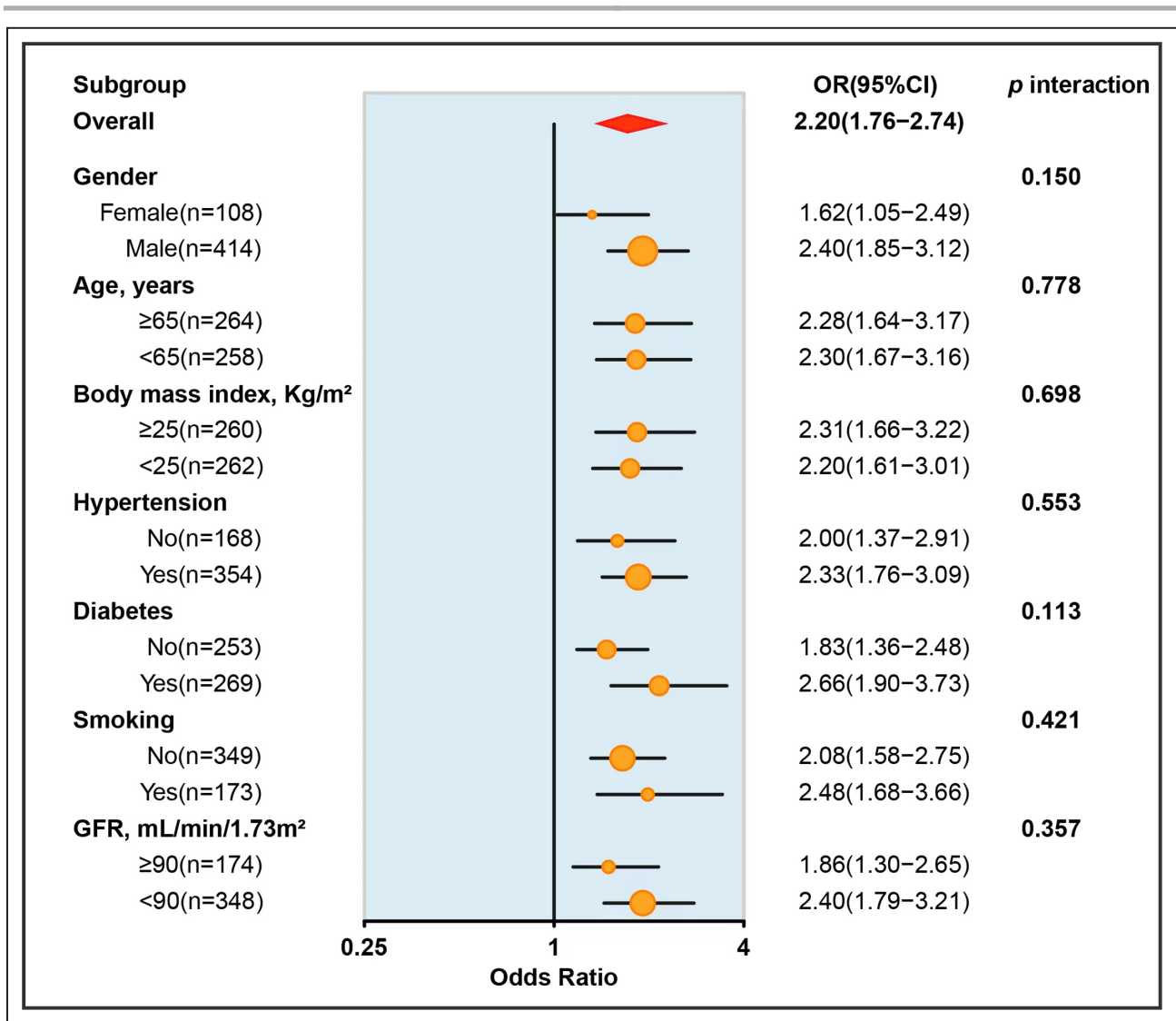


Figure 5. Adjusted ORs of poor collateralization in predefined subgroups. GFR indicates glomerular filtration rate; and ORs, odds ratios.

levels in patients with CTO with good and poor collateral formation to clarify the relationship between serpinG1 and collateral formation. The results showed that serum serpinG1 increased in the poor collateral group and correlated inversely with the Rentrop score, even after adjusting for multiple variables. Receiver operating characteristic curve analysis revealed a fair diagnostic accuracy of the serum serpinG1 level alone for detecting poor coronary collateralization. This suggests that serpinG1 may be a negative biomarker for coronary collateral formation in patients with CTO.

SerpinG1, also known as C1-inhibitor, is a member of the serine protease inhibitor gene superfamily (serpins). Serpins are an ancient superfamily of structurally similar proteins, most of which use an elegant suicide inhibition mechanism to target serine proteinases. Thirty-seven known human serpins are involved in various biological

processes, including blood coagulation, embryonic development, and extracellular matrix turnover.²⁸ Some exhibited potential angiogenesis-inhibiting properties. For example, pigment epithelium-derived factor is a secreted glycoprotein with a molecular weight of 50 kDa that blocks extracellular proliferation and angiogenesis by reducing vascular endothelial growth factor expression, partly via the suppression of oxidative stress.²⁹ Maspin, a noninhibitory member of the serpin superfamily, inhibits the migration of human endothelial cells to angiogenic factors (vascular endothelial growth factor, basic fibroblast growth factor, and interleukin-8) in a dose-dependent manner.³⁰

Similar to other serpins, serpinG1 has a serpin domain with protease inhibitory activity at the carboxy terminus, which is known to regulate coagulation, complement, and contact (kallikrein-kinin enzyme)

system activation by inhibiting the proteolytic activity of C1r and C1s. It also contains a highly glycosylated amino terminus with no homology to other serpin family members, possibly related to functions other than protease inhibition.³¹ Recent studies have found that serpinG1 exhibits robust anti-inflammatory functions both in vivo and in vitro and has the potential to antagonize COVID-19³² and sepsis. Anti-inflammatory mechanisms of serpinG1 include interactions with leukocytes to enhance phagocytosis, with endothelial cells via E- and P-selectins to interfere with leukocyte rolling and suppress transmigration of leukocytes across the endothelium, and interactions with extracellular matrix components to limit overrange activation of the complement and contact system.³³

Although there is no direct evidence that serpinG1 inhibits collateral formation, based on the known biological functions of serpinG1, including the inhibition of inflammatory cell infiltration and the ability to regulate vascular endothelial permeability, we believe that increased serpinG1 itself has the potential to inhibit collateralization. Mild inflammation is a necessary stimulus for angiogenesis or arteriogenesis, and inflammatory cells, such as neutrophils, macrophages, and mast cells, migrate to ischemic sites and release angiogenic cytokines, which is a critical step in collateral formation.³⁴ The inhibition of serpinG1 on inflammatory cell migration leads to a lack of inflammatory cells and damages the angiogenic microenvironment. In addition, the entire process of collateralization requires local and dynamic remodeling of cell-cell junctions to maintain the integrity of the neovascular sprouts.³⁵ The serpinG1 has been found to bind to extracellular matrix proteins, such as type IV collagen, laminin, and entactin,³⁶ which have the potential to reduce the adaptability of the extracellular matrix and intercellular connections, leading to endothelial cell leakage and detachment. Notably, these observations suggest that further studies are required to determine the precise role of serpinG1 in the regulation of collateral growth in patients with CTO.

Finally, serpinG1 deficiency induces hereditary angioedema, a fatal disease in which vascular permeability is briefly increased because of elevated bradykinin levels.³⁷ Both intravenous plasma-derived serpinG1 (Cinryze) and subcutaneous treatments with plasma-derived serpinG1 are approved for hereditary angioedema-targeted therapy. Therefore, this study also suggests that patients with stable coronary disease who supplement with serpinG1 for therapeutic purposes need to be more carefully assessed for their clinical benefit.

Limitations

We recognize that there are several limitations in our study. First, the study is cross-sectional for the point of coronary collateral investigation, thereby allowing us to detect associations and not predict outcomes.

Second, we evaluated the presence and degree of collateral growth according to the Rentrop scoring system. Coronary collaterals may be more accurately assessed using the collateral flow index with simultaneous measurement of aortic pressure and distal pressure within the occluded segment of the culprit coronary artery. Finally, further large-scale studies with molecular experiments are required to clarify the effect of the serpinG1 mechanism on coronary collateralization.

CONCLUSIONS

In conclusion, the present study demonstrated that *SERPING1* screened by WGCNA is associated with poor collateralization in patients with CTO. These observations might provide a rationale for improving clinical outcomes in patients with stable coronary disease and CTO. However, further studies are warranted to elucidate the specific mechanism of serpinG1 in the regulation of collateral growth in patients with CTO.

ARTICLE INFORMATION

Received July 25, 2022; accepted November 16, 2022.

Affiliations

Department of Vascular and Cardiology, Rui Jin Hospital (S.C., L.L., Z.W., F.L., K.H., Y.W., X.W., W.S., R.Z., L.L., F.D., Y.D.); and Institute of Cardiovascular Diseases (S.C., L.L., Z.W., F.L., K.H., Y.W., Q.C., X.W., W.S., Y.S., L.L., Y.D.), Shanghai Jiaotong University School of Medicine, Shanghai, China; Department of Nursing, Chongqing Medical and Pharmaceutical College, Chongqing, China (Y.L.); and Shanghai Clinical Research Center for Interventional Medicine, Shanghai, China (R.Z., F.D.).

Acknowledgments

Shuai Chen, Ying Shen, Yang Dai, Lin Lu, and Feng-Hua Ding participated in study design, data analysis and interpretation, and drafting the manuscript. Yong Liu, Zhi-Ming Wu, Le-Ying Li, Fei-Fei Li, Ke Huang, Qiu-Jing Chen, Xiao-Qun Wang, and Yi-Xuan Wang performed data collection. Rui-Yan Zhang, Lin Lu, and Wei-Feng Shen revised the manuscript before final approval. All authors read and approved the final manuscript.

Sources of Funding

This study was supported by the National Natural Science Foundation of China (81870179, 81870357, 81970362, and 81970293), Medico-engineering Research Project of Shanghai Jiao Tong University (YG2021ZD04), and Shanghai Municipal Education Commission–Gaofeng Clinical Medicine Grant Support (20181801).

Disclosures

None.

Supplemental Material

Figures S1-S3

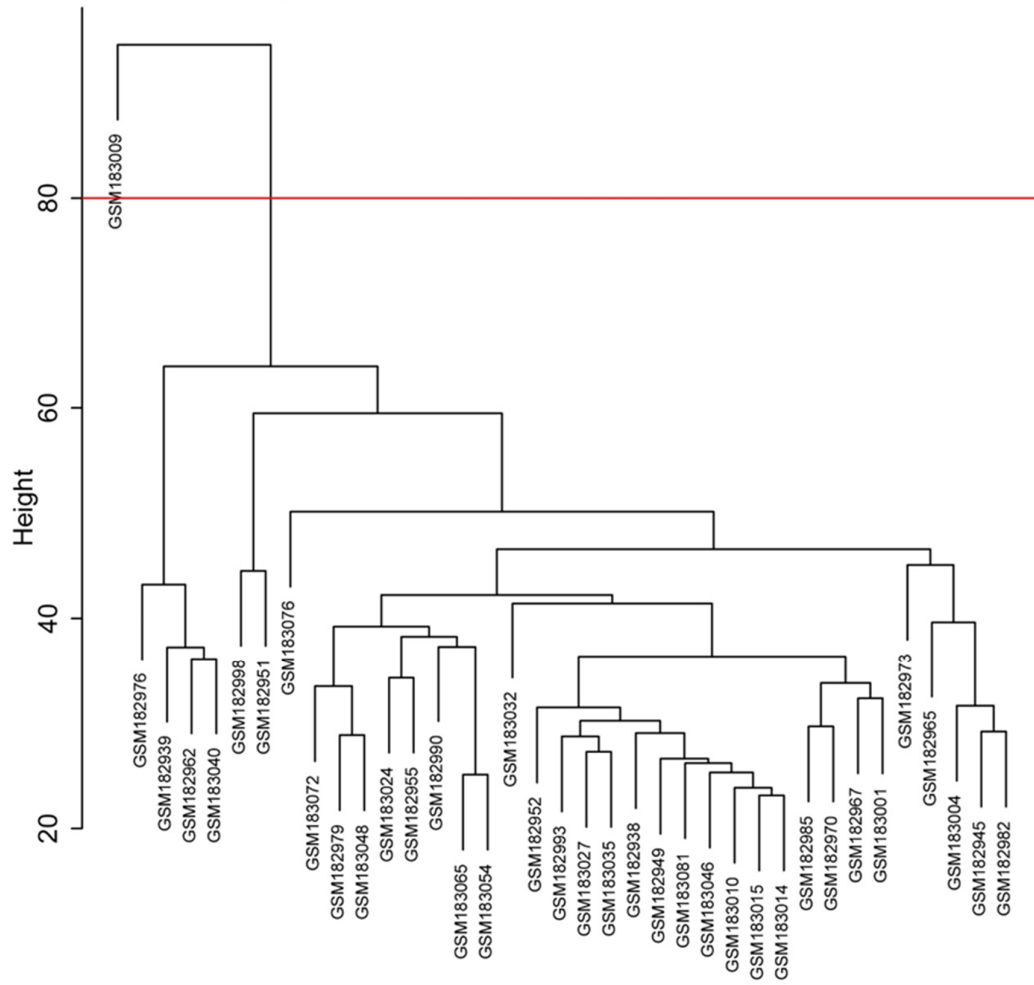
REFERENCES

1. Stone GW, Kandzari DE, Mehran R, Colombo A, Schwartz RS, Bailey S, Moussa I, Teirstein PS, Dangas G, Baim DS, et al. Percutaneous recanalization of chronically occluded coronary arteries: a consensus document: part I. *Circulation*. 2005;112:2364–2372. doi: 10.1161/CIRCULATIONAHA.104.481283
2. Jamaiyar A, Juguilon C, Dong F, Cumpston D, Enrick M, Chilian WM, Yin L. Cardioprotection during ischemia by coronary collateral growth.

- Am J Physiol Heart Circ Physiol.* 2019;316:H1–H9. doi: 10.1152/ajpheart.00145.2018
3. Shen Y, Ding FH, Dai Y, Wang XQ, Zhang RY, Lu L, Shen WF. Reduced coronary collateralization in type 2 diabetic patients with chronic total occlusion. *Cardiovasc Diabetol.* 2018;17:26. doi: 10.1186/s12933-018-0671-6
 4. Lee S, Park JM, Ann SJ, Kang M, Cheon EJ, An DB, Choi YR, Lee CJ, Oh J, Park S, et al. Cholesterol efflux and collateral circulation in chronic total coronary occlusion: effect-circ study. *J Am Heart Assoc.* 2021;10:e019060. doi: 10.1161/JAHA.120.019060
 5. Kim SH, Behnes M, Mashayekhi K, Bufo A, Meyer-Gessner M, El-Battrawy I, Akin I. Prognostic impact of percutaneous coronary intervention of chronic total occlusion in acute and periprocedural myocardial infarction. *J Clin Med.* 2021;10:258. doi: 10.3390/jcm10020258
 6. Ybarra LF, Rinfret S. Why and how should we treat chronic total occlusion? Evolution of state-of-the-art methods and future directions. *Can J Cardiol.* 2022;38:S42–S53. doi: 10.1016/j.cjca.2020.10.005
 7. Rubinshtein R, Danenberg H. Preprocedural coronary ct angiography effect on the likelihood to restore flow in chronic total occlusion. *JACC Cardiovasc Imaging.* 2021;14:2005–2007. doi: 10.1016/j.jcmg.2021.05.009
 8. Shen Y, Ding FH, Zhang RY, Zhang Q, Lu L, Shen WF. Association of serum mimecan with angiographic coronary collateralization in patients with stable coronary artery disease and chronic total occlusion. *Atherosclerosis.* 2016;252:75–81. doi: 10.1016/j.atherosclerosis.2016.07.916
 9. Shen Y, Lu L, Ding FH, Sun Z, Zhang RY, Zhang Q, Yang ZK, Hu J, Chen QJ, Shen WF. Association of increased serum glycated albumin levels with low coronary collateralization in type 2 diabetic patients with stable angina and chronic total occlusion. *Cardiovasc Diabetol.* 2013;12:165. doi: 10.1186/1475-2840-12-165
 10. Mitsos S, Katsanos K, Koletsis E, Kagadis GC, Anastasiou N, Diamantopoulos A, Karnabatidis D, Dougenis D. Therapeutic angiogenesis for myocardial ischemia revisited: basic biological concepts and focus on latest clinical trials. *Angiogenesis.* 2012;15:1–22. doi: 10.1007/s10456-011-9240-2
 11. Lavine KJ, Kovacs A, Weinheimer C, Mann DL. Repetitive myocardial ischemia promotes coronary growth in the adult mammalian heart. *J Am Heart Assoc.* 2013;2:e000343. doi: 10.1161/JAHA.113.000343
 12. Shen Y, Chen S, Dai Y, Wang XQ, Zhang RY, Yang ZK, Hu J, Lu L, Ding FH, Shen WF. Lipoprotein (a) interactions with cholesterol-containing lipids on angiographic coronary collateralization in type 2 diabetic patients with chronic total occlusion. *Cardiovasc Diabetol.* 2019;18:82. doi: 10.1186/s12933-019-0888-z
 13. Lupu IE, De Val S, Smart N. Coronary vessel formation in development and disease: mechanisms and insights for therapy. *Nat Rev Cardiol.* 2020;17:790–806. doi: 10.1038/s41569-020-0400-1
 14. Langfelder P, Horvath S. Wgcna: an R package for weighted correlation network analysis. *BMC Bioinformatics.* 2008;9:559. doi: 10.1186/1471-2105-9-559
 15. Zhang B, Horvath S. A general framework for weighted gene co-expression network analysis. *Stat Appl Genet Mol Biol.* 2005;4:Article17. doi: 10.2202/1544-6115.1128
 16. Schirmer SH, Fledderus JO, Bot PT, Moerland PD, Hoefer IE, Baan J Jr, Henriques JP, van der Schaaf RJ, Vis MM, Horrevoets AJ, et al. Interferon-beta signaling is enhanced in patients with insufficient coronary collateral artery development and inhibits arteriogenesis in mice. *Circ Res.* 2008;102:1286–1294. doi: 10.1161/CIRCRESAHA.108.171827
 17. Ritchie ME, Phipson B, Wu D, Hu Y, Law CW, Shi W, Smyth GK. Limma powers differential expression analyses for RNA-sequencing and microarray studies. *Nucleic Acids Res.* 2015;43:e47. doi: 10.1093/nar/gkv007
 18. Smyth GK. Linear models and empirical bayes methods for assessing differential expression in microarray experiments. *Stat Appl Genet Mol Biol.* 2004;3:1–25. doi: 10.2202/1544-6115.1027
 19. Yu G, Wang LG, Han Y, He QY. ClusterProfiler: an R package for comparing biological themes among gene clusters. *OMICS.* 2012;16:284–287. doi: 10.1089/omi.2011.0118
 20. Gibbons RJ, Abrams J, Chatterjee K, Daley J, Deedwania PC, Douglas JS, Ferguson TB Jr, Fihn SD, Fraker TD Jr, Gardin JM, et al. ACC/AHA 2002 guideline update for the management of patients with chronic stable angina--summary article: a report of the American College of Cardiology/American Heart Association task force on practice guidelines (committee on the Management of Patients with Chronic Stable Angina). *Circulation.* 2003;107:149–158. doi: 10.1161/01.CIR.0000047041.66447.29
 21. Rentrop KP, Cohen M, Blanke H, Phillips RA. Changes in collateral channel filling immediately after controlled coronary artery occlusion by an angioplasty balloon in human subjects. *J Am Coll Cardiol.* 1985;5:587–592. doi: 10.1016/S0735-1097(85)80380-6
 22. Levey AS, Stevens LA, Schmid CH, Zhang YL, Castro AF III, Feldman HI, Kusek JW, Eggers P, Van Lente F, Greene T, et al. A new equation to estimate glomerular filtration rate. *Ann Intern Med.* 2009;150:604–612. doi: 10.7326/0003-4819-150-9-200905050-00006
 23. Kajdacsí E, Jandrasics Z, Veszelí N, Mako V, Koncz A, Gulyás D, Kohalmi KV, Temesszentandrási G, Cervenak L, Gal P, et al. Patterns of c1-inhibitor/plasma serine protease complexes in healthy humans and in hereditary angioedema patients. *Front Immunol.* 2020;11:794. doi: 10.3389/fimmu.2020.00794
 24. Yildirim C, Nieuwenhuis S, Teunissen PF, Horrevoets AJ, van Royen N, van der Pouw Kraan TC. Interferon-beta, a decisive factor in angiogenesis and arteriogenesis. *J Interferon Cytokine Res.* 2015;35:411–420. doi: 10.1089/jir.2014.0184
 25. Schirmer SH, Bot PT, Fledderus JO, van der Laan AM, Volger OL, Laufs U, Böhm M, de Vries CJ, Horrevoets AJ, Piek JJ, et al. Blocking interferon β stimulates vascular smooth muscle cell proliferation and arteriogenesis. *J Biol Chem.* 2010;285:34677–34685. doi: 10.1074/jbc.M110.164350
 26. Teunissen PF, Boshuizen MC, Hollander MR, Biesbroek PS, van der Hoeven NW, Mol JQ, Gijbels MJ, van der Velden S, van der Pouw Kraan TC, Horrevoets AJ, et al. Mab therapy against the ifn-alpha/beta receptor subunit 1 stimulates arteriogenesis in a murine hindlimb ischaemia model without enhancing atherosclerotic burden. *Cardiovasc Res.* 2015;107:255–266. doi: 10.1093/cvr/cvv138
 27. Frangogiannis NG, Entman ML. Chemokines in myocardial ischemia. *Trends Cardiovasc Med.* 2005;15:163–169. doi: 10.1016/j.tcm.2005.06.005
 28. Lucas A, Yaron JR, Zhang L, Ambadapadi S. Overview of serpins and their roles in biological systems. *Methods Mol Biol.* 2018;1826:1–7.
 29. Matsui T, Nishino Y, Maeda S, Yamagishi S. Pedf-derived peptide inhibits corneal angiogenesis by suppressing vegf expression. *Microvasc Res.* 2012;84:105–108. doi: 10.1016/j.mvr.2012.02.006
 30. Bodenstine TM, Seftor RE, Khalkhail-Ellis Z, Seftor EA, Pemberton PA, Hendrix MJ. Maspin: molecular mechanisms and therapeutic implications. *Cancer Metastasis Rev.* 2012;31:529–551. doi: 10.1007/s10555-012-9361-0
 31. Karnaukhova E. C1-inhibitor: structure, functional diversity and therapeutic development. *Curr Med Chem.* 2022;29:467–488. doi: 10.2174/0929867328666210804085636
 32. Adesanya TMA, Campbell CM, Cheng L, Ogbogu PU, Kahwash R. C1 esterase inhibition: targeting multiple systems in covid-19. *J Clin Immunol.* 2021;41:729–732. doi: 10.1007/s10875-021-00972-1
 33. Davis AE III, Lu F, Mejia P. C1 inhibitor, a multi-functional serine protease inhibitor. *Thromb Haemost.* 2010;104:886–893. doi: 10.1160/TH10-01-0073
 34. Allahwala UK, Khachigian LM, Nour D, Ridiandres A, Billah M, Ward M, Weaver J, Bhandi R. Recruitment and maturation of the coronary collateral circulation: current understanding and perspectives in arteriogenesis. *Microvasc Res.* 2020;132:104058. doi: 10.1016/j.mvr.2020.104058
 35. Szymborska A, Gerhardt H. Hold me, but not too tight-endothelial cell-cell junctions in angiogenesis. *Cold Spring Harb Perspect Biol.* 2018;10:a029223. doi: 10.1101/cshperspect.a029223
 36. Davis AE III, Cai S, Liu D. C1 inhibitor: biologic activities that are independent of protease inhibition. *Immunobiology.* 2007;212:313–323. doi: 10.1016/j.imbio.2006.10.003
 37. Busse PJ, Christiansen SC. Hereditary angioedema. *N Engl J Med.* 2020;382:1136–1148. doi: 10.1056/NEJMra1808012

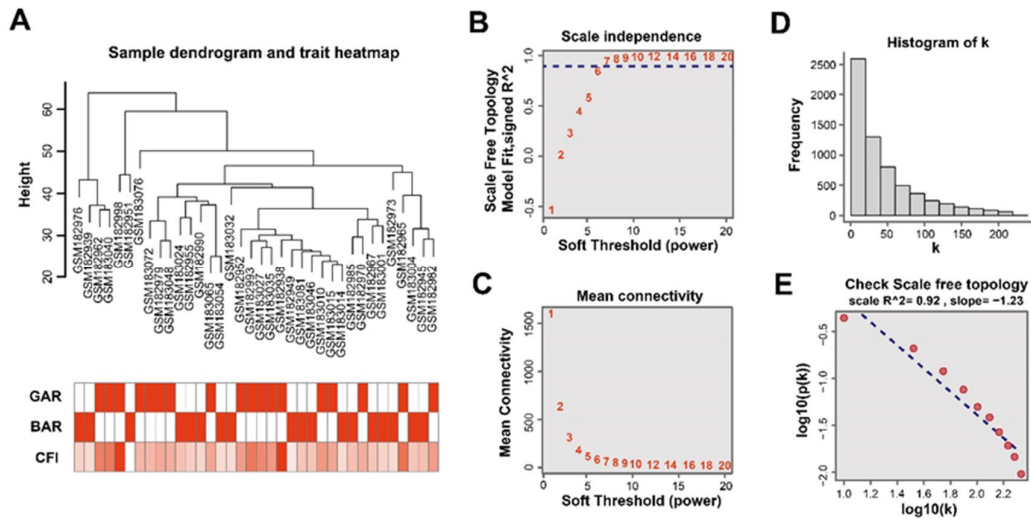
SUPPLEMENTAL MATERIAL

Figure S1. Sample clustering to detect outliers



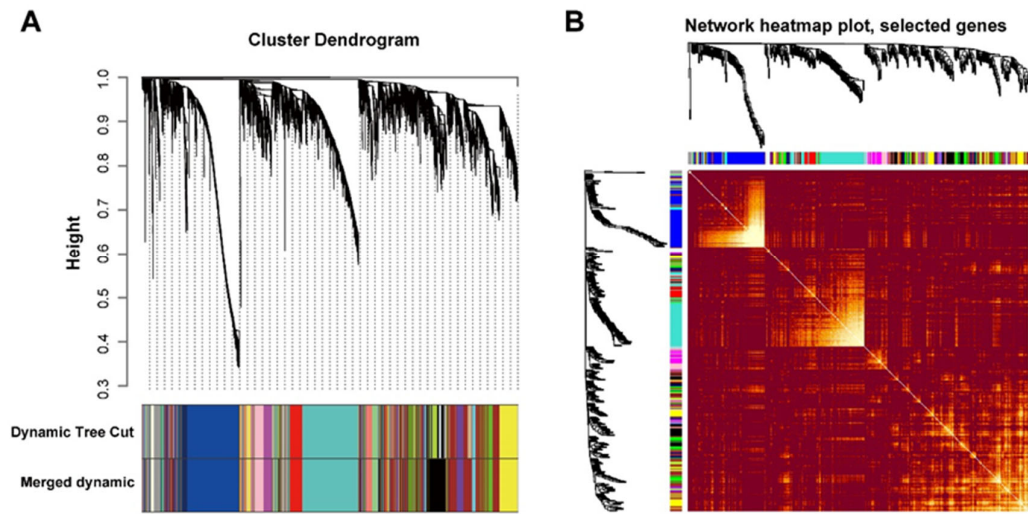
One outlier sample was excluded from our further analysis.

Figure S2. Clustering of samples and determination of soft thresholding power



(A) Sample dendrogram and trait heatmap. The clustering analysis was based on the expression data of GSE7547, which contains of 18 good arteriogenic responders (GARs) and 18 bad arteriogenic responders (BARs). (B) Analysis of scale-independence index for various soft threshold powers. (C) Analysis of mean connectivity for various soft threshold powers. (D) The histogram of k of the samples. (E) The correlation coefficient between k and $p(k)$ of the samples, and the R^2 reached 0.9. BAR, bad arteriogenic responders; CFI, collateral flow index; and GAR, good arteriogenic responders.

Figure S3. Construction of co-expression modules by the weighted gene co-expression network analysis (WGCNA) package in R



(A) Clustering dendrograms of genes. Each branch in the diagram represents a gene, and each color below represents a co-expression module. We got an aggregate of 16 co-expression modules for further analysis. (B) A topological overlap matrix (TOM) was built to analyze the independence among the 16 co-expression modules. In the heatmap, a light color indicated high overlap, while dark colors indicate low overlap.